Int. J. Solids Structures Vol. 28, No. 9, pp. 1185–1197, 1991
Printed in Great Britain.

0020–7683/91 $3.00 + .00

NON-LINEAR FLEXURE TESTING OF A HIGH-STRENGTH GLASS DISK

M. INOUE, Y. TAKIZAWA and A. OKADA
Corning Japan K.K., Shizuoka Operations Center, Technical Center, 12117, Ohbuchi, Osuka-cho, Ogasa-gun, Shizuoka 437-13, Japan

(*Received* 16 *July* 1990; *in revised form* 15 *March* 1991)

Abstract—Strength measurements of glass disk substrates were made by ring-on-ring flexural testing. The non-linear problem of a disk undergoing a large deflection in ring bending was solved approximately by a variational method. The solution has the minimum total energy and satisfies the required boundary conditions. Deflection, stress and strain distributions are evaluated as functions of the external load in terms of seven parameters related to sample material and geometry. Good agreement between experiment and theory has been obtained without any adjustable parameter for a glass disk of Corning Code 0313.

NOTATION

D	flexural rigidity $= [Et^3/12(1-\nu^2)]$
Δ	Div. Grad.
E	Young's modulus
F	free energy
ν	Poisson's ratio
μ	$1+\nu/1-\nu$
P	total load
q	intensity of load
R_I	inner radius of a disk
R_O	outer radius of a disk
R_L	loading radius
R_S	supporting radius
T	total energy
t	thickness of a disk
χ	stress function
w	deflection
M_r, M_t	bending moment
σ_r, σ_t	stress
ε_r, ε_t	strain.

Subscripts r and t refer to the radial and tangential (hoop) components, respectively.

1. INTRODUCTION

Glass is widely used as a substrate material of many devices. Mechanical strength of glass is often a key factor in determining such applications. High-strength glasses are required particularly for disk substrate. Glass is strengthened by chemical tempering which exchanges the alkaline ions by ions of larger size. This induces surface compression of 40–60 kg mm^{-2} in a glass disk and makes the disk resistant to the external stresses by freezing surface flaws (Bartholomew and Garfinkel, 1980).

A common method to measure the strength of glass is the modulus of rupture (MOR) by which the maximum of the failure stress under external loading is determined. The failure load is dependent upon geometry of a sample and the measurement as well as on the material parameters. In ring flexural testing in which a sample disk is pressed between two concentric rings of different diameters strengthened glass usually undergoes a deflection more than three times the disk thickness before it breaks. When the deflection is larger than half of the disk thickness, the disk is deformed so as to change an area of its mid-plane (Landau and Lifshitz, 1973). There is no neutral plane. In this case both bending and stretching stresses come into play. This problem essentially involves a non-linear effect and therefore cannot be analyzed by a linear elastic theory which is used for small deflection

analysis. The non-linear effect occurs especially in the case of two-dimensional deformation as in the ring bending of a disk. In contrast, for the case of one-dimensional or uniaxial bending, such as deformation of a bar or a rectangular plate into a cylindrical surface, a large deflection with a neutral plane is induced by bending without stretching and is described by a linear modelling appropriately.

A non-linear stress analysis for a disk in different geometries has been reported by various authors. Earlier works were reviewed in the book of Timoshenko and Woinowsky-Krieger (1959). For ring-bending of a glass disk numerical solutions of the non-linear equations were obtained by Kao *et al.* (1971) for a solid disk. Connolly *et al.* (1989) did the strength analysis of an annular disk using the finite element method.

In this paper we present the strength analysis of a high-strength glass disk under ring bending using a variational method. This method makes it relatively easy to evaluate analytically the physical variables in terms of the material and geometrical parameters of the system. The experimental set-up and procedures are described in Section 2. The deflection and the strains of radial and tangential components are measured for samples of a Corning Code 0313 glass disk on a ring-on-ring fixture in a universal test machine. The non-linear problem of large deflection of a disk is solved by using a variational method in Section 3. A solution of the minimum total energy satisfying the imposed boundary conditions is analytically derived. Deflection, stress and strain distributions are given as a function of the external load in terms of the seven parameters that are related to the material, sample size and geometry of the test fixture. Theoretical and experimental results are compared to determine the strength of a glass disk in Section 4.

2. EXPERIMENTAL PROCEDURE

2.1. *Samples*

The samples used in this experiment are annular glass disks made of Corning Codes 0313 and 0317 glasses. Code 0313 glass is strengthened from Code 0317 by chemical tempering and is commercially used as a substrate for memory disks. The material and geometrical parameters of the samples are listed in Table 1.

2.2. *Measurements*

The ring-on-ring flexural test was done with the INSTRON 4206 universal test machine. The experimental set-up is illustrated schematically in Fig. 1. A disk specimen is placed on a supporting ring. The pressure is applied normally to the disk by pushing a loading ring slowly. The loading ring has a diameter of 25 mm and the supporting ring has a diameter of 110 mm. Both rings are made of stainless steel and have polished semi-circular cross-sections of 5 mm radius in contact with the sample disk. Deflection at the loading radius is directly measured from the crosshead displacement. Radial and tangential components of strain at five fixed radial points on the disk are measured simultaneously by Kyowa bi-axial strain gauges glued on the lower surface of the disk. Deflection, load and strain data are

Table 1. Values of parameters

		Material parameters						
		Code 0313 glass		Code 0317 glass				
	E	7300 kg mm^{-2}		7400 kg mm^{-2}				
	ν	0.22		0.22				
Sample parameters								
ϕ (mm)	R_I (mm)	R_O (mm)	R_L (mm)	R_S (mm)	t (mm)	SC (kg mm^{-2})	DOL (μm)	
130	7.5	65.0	12.5	55.0	1.2	45	94	

SC, surface compression; DOL, depth of layer.

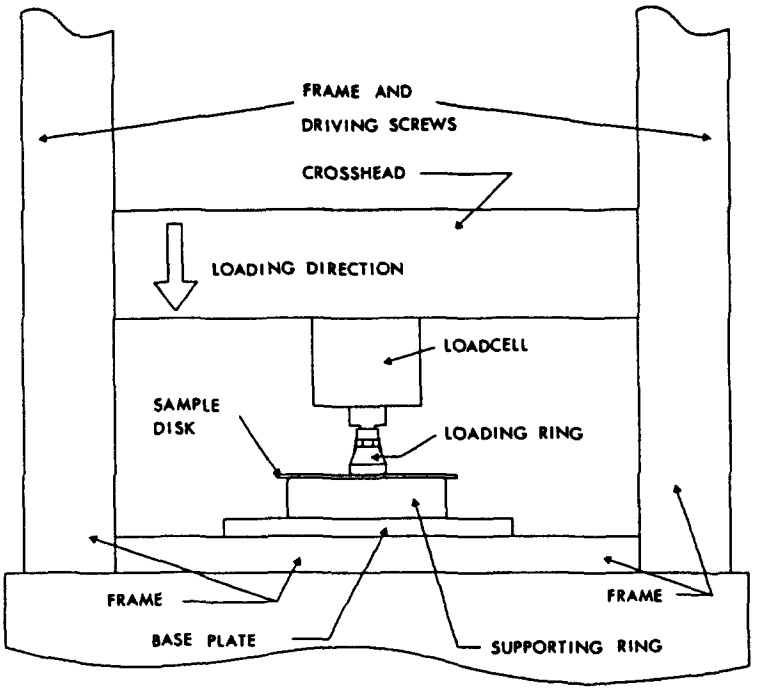

Fig. 1. Experimental setup of the ring flexural test.

taken at 1 s intervals while increasing the applied load up to the failure load, with a crosshead speed of 1.5 mm min^{-1}. Data acquisition is automated by an HP86B and a VAX-11/730 computer.

3. THEORETICAL ANALYSIS

When an elastic plate has a large deflection it is deformed by both bending and stretching of the mid-plane so that the equilibrium state of the deformed disk is attained, so as to minimize the strain energy of the plate due to bending and stretching under the external load.

Analyzing a disk with large deflection is essentially a non-linear problem to which the linear theory of small deflection is not applicable (Landau and Lifshitz, 1973). Here we will solve the non-linear problem approximately by using the variational method which gives a solution with the minimum total energy with respect to a deflection parameter.

Let us consider a disk with a central circular hole whose thickness is much smaller than the diameter. Then, for circularly symmetrical deformation of the disk, we can use the plane stress approximation neglecting the shearing stresses and the stress component along the thickness.

The free energy of a disk under large deflection is given by

$$F = V_1 + V_2 \tag{1}$$

where the first term V_1 represents the strain energy due to pure bending of a plate and the second term V_2 the stretching energy of the mid-plane. The energy terms are expressed in terms of radial and tangential components by

$$V_1 = -\pi \int_{R_1}^{R_0} \left\{ M_r \frac{d^2 w}{dr^2} + M_t \frac{1}{r} \frac{dw}{dr} \right\} r \, dr, \tag{2}$$

$$V_2 = \pi t \int_{R_1}^{R_0} \{\sigma_r^s \varepsilon_r^s + \sigma_t^s \varepsilon_t^s\} r \, dr, \tag{3}$$

where the superscript s refers to stretching.

The potential energy due to the applied load is given by

$$U = -2\pi \int_{R_I}^{R_O} qwr \, dr. \tag{4}$$

Assuming that the loading ring has a sharp edge contact with the disk, the load intensity q is approximated by a delta function

$$q = \frac{P}{2\pi R_L} \delta(r - R_L). \tag{5}$$

The total energy, $F+U$, becomes minimal in the equilibrium state, so that the variation of the total energy, δT, is zero:

$$\delta T = \delta V_1 + \delta V_2 + \delta U = 0. \tag{6}$$

Relation (6) leads to coupled non-linear equations for deflection and stress tensors.

Here we apply a variational method to solve eqn (6) analytically. Following the method used by Timoshenko and Woinowski-Krieger (1959), we introduce a trial function for deflection which satisfies the boundary conditions for a disk under ring bending and includes one parameter,

$$w_i = w0(A_i + B_i r^2 + C_i \log r + D_i r^2 \log r), \quad i = \begin{cases} 1 \text{ for } R_I < r < R_L \\ 2 \text{ for } R_L < r < R_S \\ 3 \text{ for } R_S < r < R_O, \end{cases} \tag{7}$$

where the coefficients A_i, B_i, C_i and D_i are determined by geometrical and material parameters of the disk as given by (A6) in Appendix A. The displacement field of a circular disk for small deflection in the ring bending is represented by eqn (7) with the coefficients which vary linearly with the applied load (Roark and Young, 1982). Thus, this trial function extrapolates naturally to the linear solution of displacement field in the limit of small deflection. We will evaluate the unknown parameter $w0$ from the condition of minimum energy (6).

It is convenient to introduce a stress function for this purpose, as calculated in Appendix B. Then, the radial and tangential stresses due to stretching are given in terms of the stress function by

$$\sigma_r^i = \frac{1}{r}\frac{\partial \chi}{\partial r} = P_i + \frac{Q_i}{r^2} - \frac{E}{2r^2} G_i(r), \tag{8}$$

$$\sigma_t^i = \frac{\partial^2 \chi}{\partial r^2} = P_i - \frac{Q_i}{r^2} + \frac{E}{2}\left[\frac{1}{r^2} G_i(r) - F_i(r)\right], \tag{9}$$

$$i = 1, 2, 3$$

where the functions $F_i(r)$ and $G_i(r)$ are given by eqns (B4) and (B3), respectively, and the coefficients P_i and Q_i are given by eqn (B6) in Appendix B. Integrating by parts each of the three terms in eqn (6) with the boundary conditions, so that the bending moment and the shearing force vanish at the inner and outer edges of a disk, we obtain the minimum energy condition

$$\left\{\int_{R_I}^{R_L}\delta_{i1}+\int_{R_L}^{R_S}\delta_{i2}+\int_{R_S}^{R_O}\delta_{i3}\right\}\left[D\frac{\mathrm{d}(\Delta w_i)}{\mathrm{d}r}-t\frac{1}{r}\frac{\partial\chi}{\partial r}\frac{\mathrm{d}w_i}{\mathrm{d}r}-\frac{P}{2\pi r}\delta_{i2}\right]\frac{\mathrm{d}(\delta w_i)}{\mathrm{d}r}r\,\mathrm{d}r=0, \tag{10}$$

where δ_{ij} is Kronecker's delta. As detailed in Appendix B, the above integral is evaluated to be

$$DC1w0+tC3(w0)^3+PC0=0, \tag{11}$$

where the parameters $C0$, $C1$ and $C3$ are given by (B8).

In eqn (11) the linear term in $w0$ comes from the bending energy [eqn (2)], the third order term from the stretching [eqn (3)] and the constant term from the potential energy of the external load [eqn (4)]. The equation has a real solution which is given by

$$w0=[(a_1^3+a_0^2)^{1/2}+a_0]^{1/3}-[(a_1^3+a_0^2)^{1/2}-a_0]^{1/3}, \tag{12}$$

with

$$a_0=-\frac{P}{2t}\frac{C0}{C3}, \tag{13}$$

and

$$a_1=\frac{D}{3t}\frac{C1}{C3}, \tag{14}$$

where $a_1^3+a_0^2>0$ and $a_1>0$. The radial and tangential stresses due to pure bending at the lower face of the disk are obtained from the moment by

$$\sigma_r^b=\frac{6M_r}{t^2}=-\frac{6Dw0}{t^2}\left[2(1+\nu)B_i-\frac{(1-\nu)}{r^2}C_i+(3+\nu)D_i+2(1+\nu)D_i\log r\right], \tag{15}$$

and

$$\sigma_t^b=\frac{6M_t}{t^2}=-\frac{6Dw0}{t^2}\left[2(1+\nu)B_i+\frac{(1-\nu)}{r^2}C_i+(1+3\nu)D_i+2(1+\nu)D_i\log r\right], \tag{16}$$

where the superscript b refers to bending. The total stress is given by a sum of bending and stretching stresses:

$$\sigma_r=\sigma_r^b+\sigma_r^s, \tag{17}$$

$$\sigma_t=\sigma_t^b+\sigma_t^s. \tag{18}$$

For elastic materials like glasses the strain is related to the stress by

$$\varepsilon_r=\frac{1}{E}(\sigma_r-\nu\sigma_t), \tag{19}$$

$$\varepsilon_t=\frac{1}{E}(\sigma_t-\nu\sigma_r). \tag{20}$$

The present approximation not only gives the results of the linear theory for small deflection

in the small external load as mentioned before, but also describes dependence of deflection, stress and strain upon P and the disk thickness t for large deflection. We can easily find the asymptotic behaviors of these quantities for very small and very large values of P. Equation (11) leads to $w0 \simeq -P(C0\,DC1)$ in the limit of small deflection which is proportional to Pt^{-3}. For very large deflection, on the other hand, $w0$ is given approximately by $(-PC0/tC3)^{1/3}$ which makes deflection proportional to $(P/t)^{1/3}$. The stress and strain due to bending increase like Pt^{-2} with small P as in the linear theory but they change like $P^{1/3}t^{2/3}$ for very large values of P. On the other hand, stress and strain due to stretching, which vary with $(w0)^2$, increase like P^2t^{-6} with small P and like $(P/t)^{2/3}$ with large P.

4. RESULTS

In this section we present and discuss the experimental and theoretical results for Corning Code 0313 disks with a 130 mm diameter and 1.2 mm thickness. Values of the related parameters are listed in Table 1.

4.1. *Deflection*

Calculated distribution of deflection is plotted for different values of load in Fig. 2. The overall deflection between the two edges of a disk is several times larger than the thickness.

Figure 3 shows the experimental and theoretical curves of deflection versus the external load at constant radii. A very good agreement between theory and experiment was obtained for the curve at the loading radius. Deflection increases linearly with P for small values of P and then much more slowly as P increases. One can see that there is an appreciable deviation from the linear theory as the deflection exceeds roughly one half of the thickness.

4.2. *Strain*

Radial and tangential (hoop) strains have been directly measured at $r = 9.0$, 12.5, 22.5, 40.0 and 62.5 mm by varying the external load. The experimental and theoretical values of strain distribution are presented in Fig. 4. The tangential component of strain is larger than the radial component in the inner half radii of the disk and increases rapidly toward the maximum value at the inner edge of a disk. The calculated radial strain has a maximum

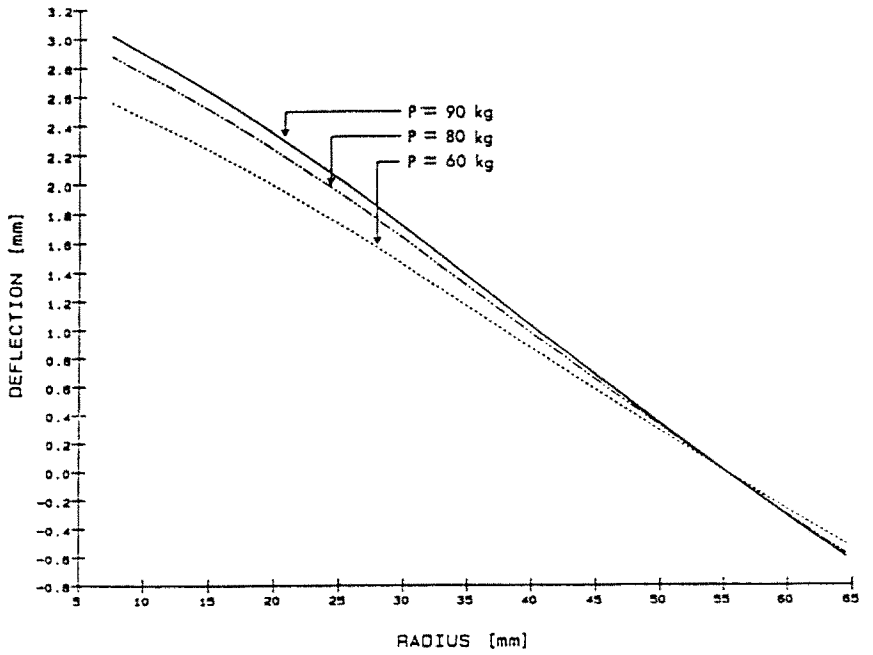

Fig. 2. Theoretical deflection distribution at constant loads.

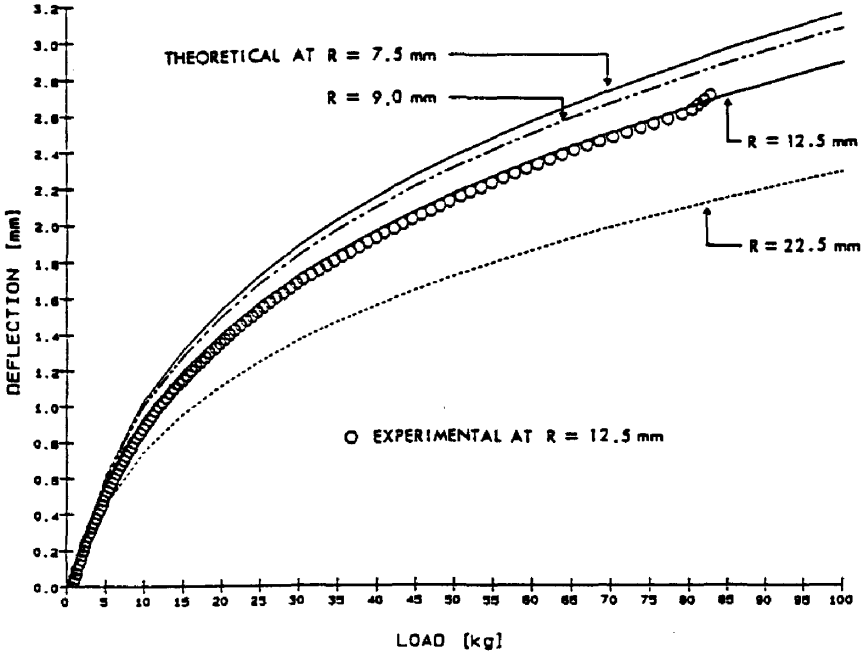

Fig. 3. Deflection vs load at constant radii.

roughly at $R = 15$ mm from which it decreases rapidly toward the inner radius but gradually toward the outer radius. The theory reproduces the observed strain distribution in the disk fairly well with some discrepancies in the vicinity of the loading ring and the outer radius, as will be discussed below.

Figures 5a, 5b and 6 show the radial and tangential strain curves as a function of the external load P, respectively. The strain increases linearly with P in the beginning and then much more slowly as P becomes larger. The slope of the tangential strain distribution near the inner edge of a disk for large P is about 5×10^{-4} mm^{-1}. A drop in the observed strain

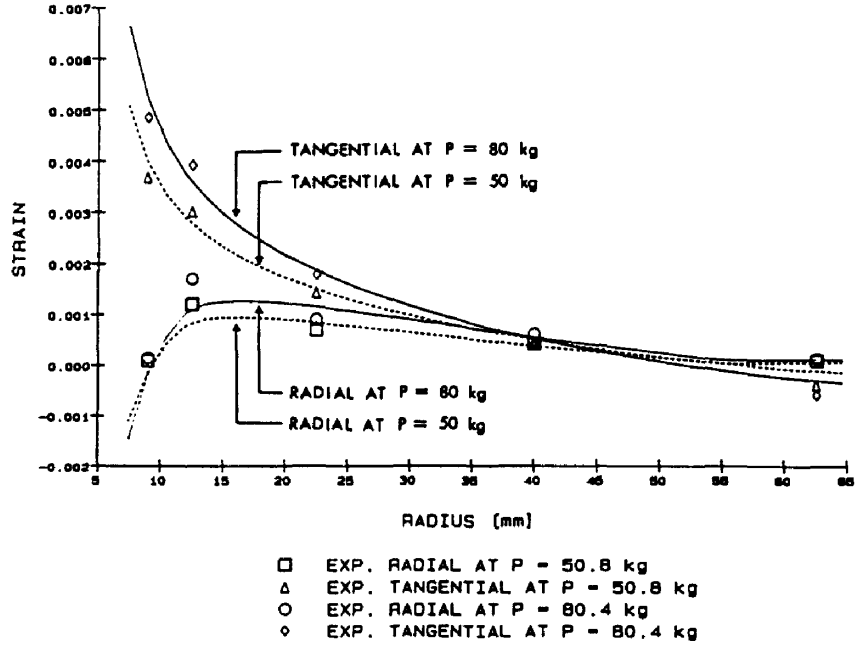

Fig. 4. Strain distribution at constant loads.

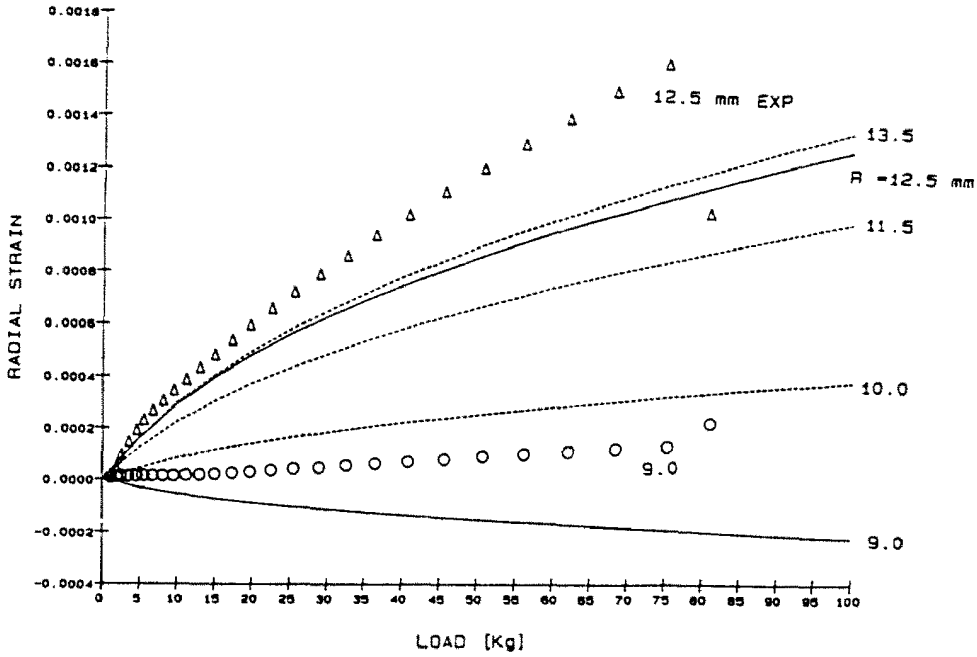

Fig. 5(a). Radial strain vs load at constant radii.

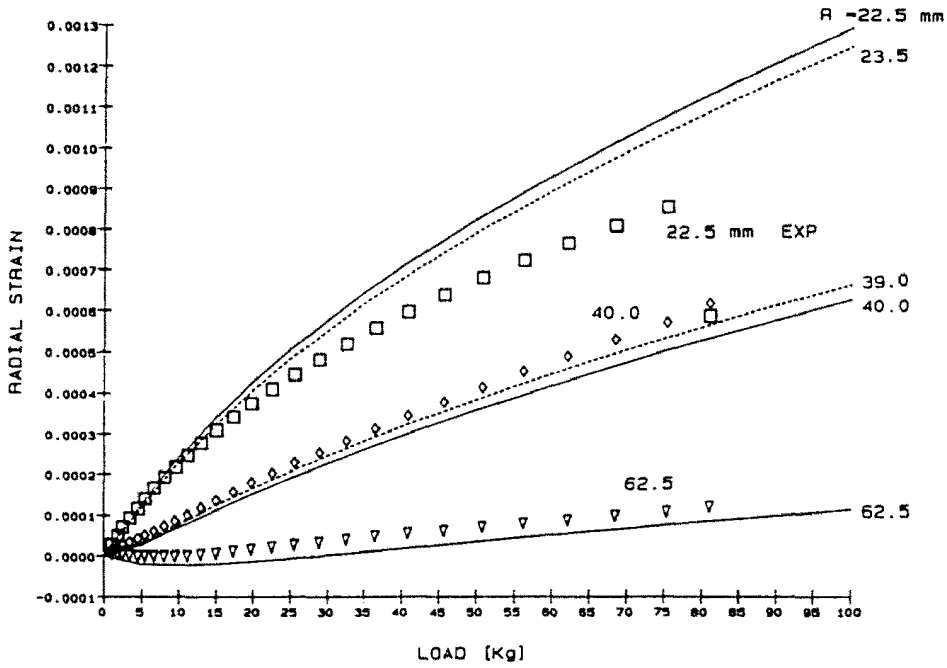

Fig. 5(b). Radial strain vs load at constant radii.

curve near 80 kg is caused by partial detachment of a strain gauge from the disk when the external load is close to the failure load.

The instrumental error for the measurement is estimated to be $\pm 2\%$. In addition, the limit of accuracy in positioning the strain gauge on the disk face is about ± 1 mm in length and $\pm 3°$ in angle in the present experiment. If the strain gauge is misaligned $\pm 3°$ in angle, for instance, the observed radial strain component is increased or decreased roughly in the order of 3% of the tangential component while the tangential component is decreased or increased in the order of 3% of the radial component. The discrepancies between theory

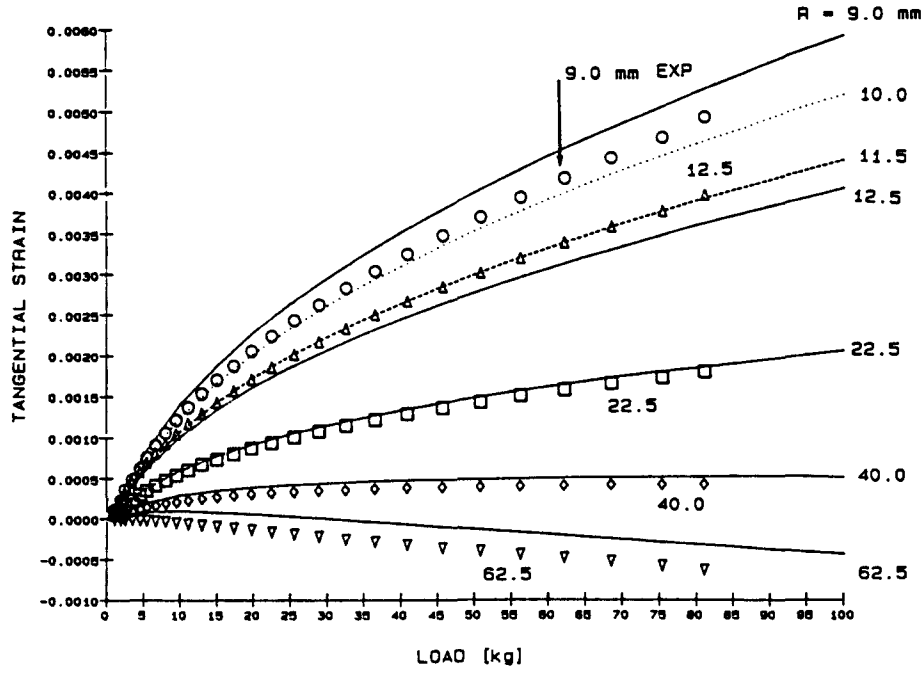

Fig. 6. Tangential strain vs load at constant radii.

and experiment at $R = 9.00$ and 40.0 mm as shown in Figs 5 and 6 are within the experimental errors. On the other hand, the observed radial strains at $R = 12.5$ and 22.5 mm, which are located before and after the theoretical maximum point, respectively, deviate from the theory beyond the experimental errors in magnitude and in sign. The observed tangential strain at $R = 60.5$ mm also deviates from the theoretical curve more than the experimental error in Fig. 6.

4.3. *Stress*

We now look at the total stress which is commonly used to determine the strength of the material. Figure 7 gives a plot of stress distribution at constant loads. The tangential

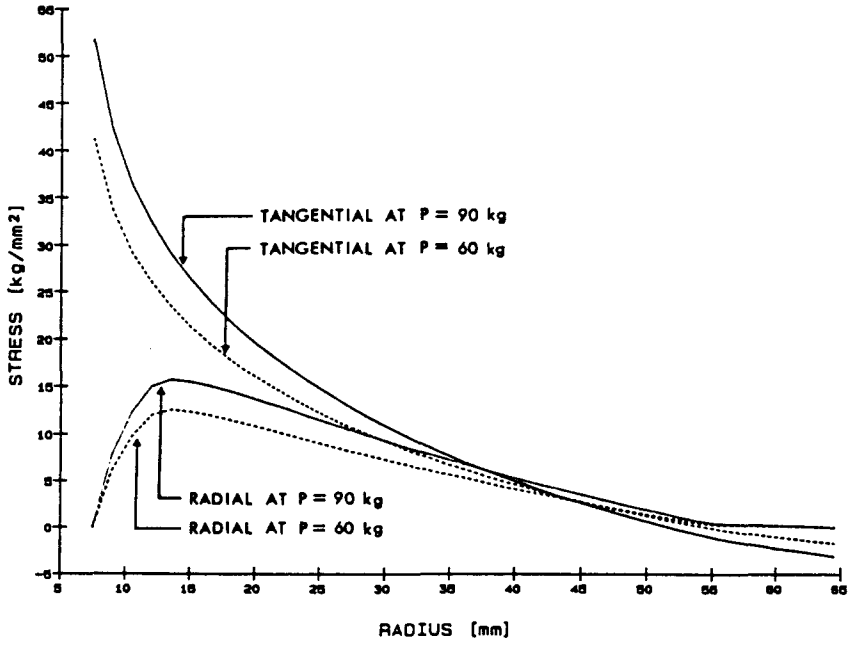

Fig. 7. Theoretical stress distribution at constant loads.

stress is tensile at the inner edge of the disk and decreases monotonically to be compressive at the outer edge. On the other hand, the radial stress increases rapidly from zero to the maximum between the inner edge and the loading radius, and then decreases gradually toward the outer radius of the disk.

Figure 8 shows the tangential stress of bending and that of stretching at the inner edge of a disk as functions of P. The bending stress increases linearly with P up to $P = 5$ kg whereas the stretching stress varies like P^2. As P increases the stretching stress increases more rapidly like $P^{2.3}$ than the bending stress which varies like $P^{1.3}$.

In Fig. 9 radial and tangential stresses are plotted versus the external load at fixed radii. Deviation from the linear relation between stresses and P is again significant for a wide range of P.

It is known that fracture of a brittle material like glass occurs when the maximum tensile stress becomes equal to the strength of the material. Our experiment has shown that the fracture of a sample disk in this type of test always originates at the inner edge. The strength can be estimated from the curve of Fig. 8 for the observed failure load of 80 kg. The strength value so determined is 49 kg mm^{-2}. On the other hand, the strength of Code 0313 glass is roughly given by a sum of the strength of untreated glass (Code 0317) and the surface compression produced by chemical tempering. The strength of untreated glass measured by a ring flexural test is about 15 kg mm^{-2} on the average for a 130 mm disk. The surface compression due to chemical tempering is 45 kg mm^{-2} as measured by the optical method (Kishii, 1979). Thus the expected strength of Code 0313 glass is 60 kg mm^{-2} which is larger than the strength estimated from our ring flexural test, and predicts a failure load of 118 kg.

5. DISCUSSION

Our results show that a high-strength disk under ring bending experiences a large deflection and is properly described by the non-linear theory. A variational method was applied to solve the non-linear problem approximately. The solution has the minimum total energy with respect to a deflection parameter and meets the required boundary conditions. The neglect of the shearing stresses, τ_{rz} and $\tau_{\theta z}$, and the stress component σ_{zz} are well justified in the present case where the ratio of the thickness to the outer radius of the disk is as small

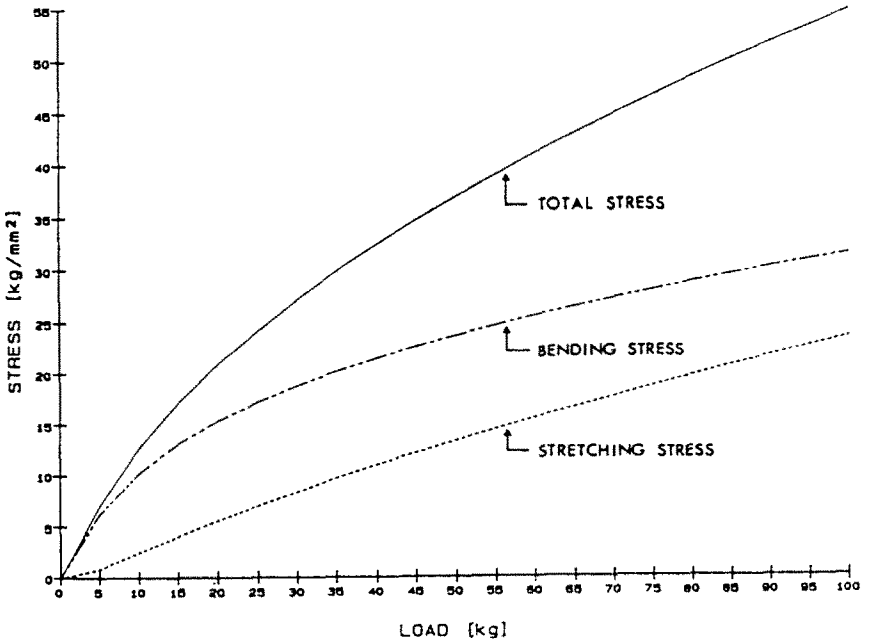

Fig. 8. Theoretical maximum tangential stress vs load at inner radius, $R = 7.5$ mm.

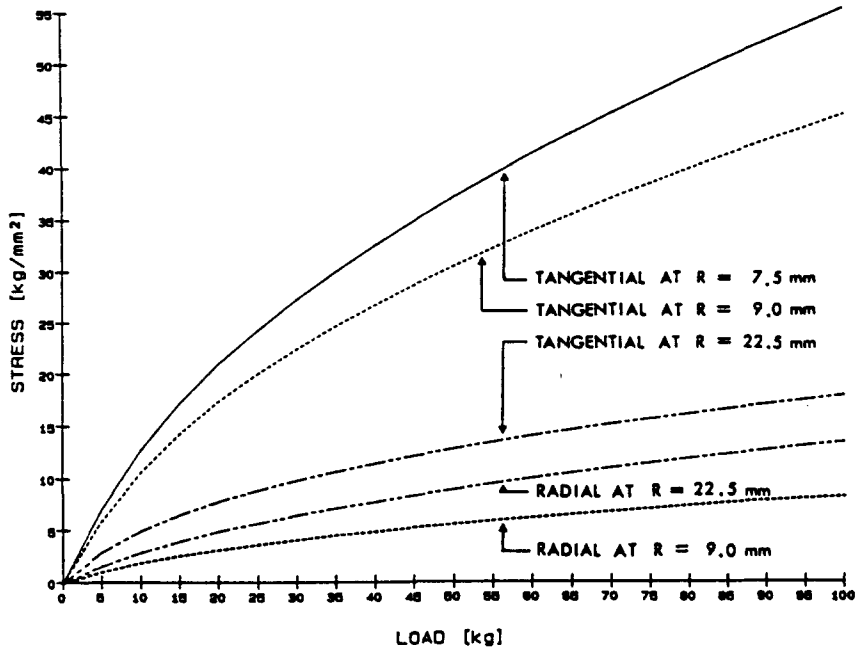

Fig. 9. Theoretical stress vs load at constant radii.

as 0.02; as discussed in detail by Timoshenko and Woinowski-Krieger (1959) and Love (1906). Good agreement between theory and experiment, without any adjustable parameter, in deflection versus load indicates that our solution adequately approximates the real solution. The theory also explains the observed distribution and load dependence of strain satisfactorily within experimental error. However, the observed radial strain distributions at 12.5 mm are more than 10% larger, and those at 22.5 mm are likewise smaller than, the theoretical predictions. In the actual set-up of the ring flexural test, the loading and supporting rings have a semi-circular edge which has a finite surface of contact with a disk instead of a sharp edge contact used in our model calculations. This leads to a slight reduction of the theoretical tensile stress at the lower face of the disk under the loading ring and therefore gives additional discrepancy of the experimental results from the theory (Timoshenko and Woinowski-Krieger, 1959). The stress magnification of a disk under the loading ring was reported in the experimental works by Rosenfield (1979) and reproduced by the finite element analysis of Ritter *et al.* (1980).

Acknowledgements—The authors are indebted to F. L. Thiel and M. Teter for comments on and reviewing of the manuscript, and to S. T. Gulati, J. D. Helfinstine, K. Minematsu and Y. Wada for providing information on various subjects in this paper.

REFERENCES

Bartholomew, R. F. and Garfinkel, H. M. (1980). Chemical strengthening of glass. *Glass. Sci. Technol.* **5**, 217–270.

Connolly, D., Stockton, A. C. and O'Sullivan, T. C. (1989). Large-deformation strength analysis of chemically strengthened glass disk. *J. Am. Ceram. Soc.* **72**, 859–863.

Kao, R., Perrone, N. and Capps, W. (1971). Large-deflection solution of the coaxial-ring-circular-glass-plate flexure problem. *J. Am. Ceram. Soc.* **54**, 566–571.

Kishii, J. (1979). Surface stress measurement using optical waveguide effect of chemically tempered glass. *Yogyo-Kyokai-shi* **87**, 119–126. (In Japanese).

Landau, L. D. and Lifshitz, E. M. (1973). *Theory of Elasticity*. Pergamon Press, Oxford.

Love, A. E. H. (1906). *Mathematical Theory of Elasticity*. Cambridge Univ. Press, Cambridge.

Ritter, J. E., Jr, Jakus, K., Batakis, A. and Bandyopadhyay, N. (1980). Appraisal of biaxial strength testing. *J. Non-Cryst. Solids* **38 & 39**, 419–424.

Roark, R. J. and Young, W. C. (1982). *Formulas for Stress and Strain*. McGraw-Hill, New York.

Rosenfield, A. R. (1979). Failure of ceramics under multiaxial stresses. *Third Quarterly Report*. Battelle, Columbus Lab.

Timoshenko, S. P. and Woinowsky-Krieger, K. (1959). *Theory of Plates and Shells*. McGraw-Hill, New York.

APPENDIX A

We calculate a trial function for deflection which satisfies a linear homogeneous equation

$$\Delta^2 w = 0, \tag{A1}$$

and the boundary conditions

$$M_r = -D\left(\frac{d^2w}{dr^2} + \frac{\nu}{r}\frac{dw}{dr}\right) = 0 \quad \text{at} \quad r = R_I \quad \text{and} \quad R_O, \tag{A2}$$

$$Q_r = -D\frac{d}{dr}(\Delta w) = 0 \quad \text{at} \quad r = R_I \quad \text{and} \quad R_O, \tag{A3}$$

$$w = 0 \quad \text{at} \quad r = R_S. \tag{A4}$$

We look for a general solution of eqn (A1) separately for three regions of radius as expressed by

$$w = w0(A_i + B_i r^2 + C_i \log r + D_i r^2 \log r), \quad i = \begin{cases} 1 \text{ for } R_I \leqslant r \leqslant R_L \\ 2 \text{ for } R_L \leqslant r \leqslant R_S \\ 3 \text{ for } R_S \leqslant r \leqslant R_O. \end{cases} \tag{A5}$$

As deflection and moment must be continuous in the whole disk w, dw/dr and d^2w/dr^2 are continuous at $r = R_L$ and R_S.

The coefficients A_i, B_i, C_i and D_i in eqn (A5) are determined so as to satisfy the five boundary conditions, (A2)–(A4) and the six continuity conditions. The coefficients are given by

$$\begin{aligned}
A_1 &= A_2 + (B_2 - B_1)R_L^2 + (C_2 - C_1)\log R_L + D_2 R_L^2 \log R_L, \\
B_1 &= \frac{1}{R_O^2 - R_I^2}\left[R_O^2 \log\left(\frac{R_L}{R_S}\right) - \frac{1}{2\mu}(R_S^2 - R_L^2)\right], \\
C_1 &= 2\mu R_I^2 B_1, \\
D_1 &= 0, \\
A_2 &= -B_2 R_S^2 - C_2 \log R_S - D_2 R_S^2 \log R_S, \\
B_2 &= -\frac{1}{R_O^2 - R_I^2}\left[R_O^2 \log R_S - R_I^2 \log R_L + \frac{(R_S^2 - R_L^2)}{2\mu}\right] - 1, \\
C_2 &= \frac{2\mu R_I^2 R_O^2}{R_O^2 - R_I^2}\left[\log\left(\frac{R_L}{R_S}\right) + \frac{1}{2\mu}\left\{\left(\frac{R_L}{R_I}\right)^2 - \left(\frac{R_S}{R_O}\right)^2\right\}\right], \\
D_2 &= 1, \\
A_3 &= -B_3(R_S^2 + 2\mu R_O^2 \log R_S), \\
B_3 &= \frac{1}{R_O^2 - R_I^2}\left[R_I^2 \log\left(\frac{R_L}{R_S}\right) - \frac{1}{2\mu}(R_S^2 - R_L^2)\right], \\
C_3 &= 2\mu R_O^2 B_3, \\
D_3 &= 0.
\end{aligned} \tag{A6}$$

APPENDIX B

In the absence of the external radial force, the stress due to stretching is induced by bending. The stress function in this case satisfies the differential equation

$$\frac{\partial}{\partial r}(\Delta\chi) = -\frac{E}{2r}\left(\frac{dw}{dr}\right)^2. \tag{B1}$$

Integrating the above equation with trial function (A5) we have

$$\frac{\partial\chi}{\partial r} = P_i r + \frac{Q_i}{r} - \frac{E}{2r}G_i(r), \tag{B2}$$

where subscripts i refer to each of the three regions defined in eqn (A5) in Appendix A. The function $G_i(r)$ is given by an indefinite integral

$$G_i(r) = \int r F_i(r)\, dr, \tag{B3}$$

with

$$F_i(r) = \int \frac{1}{r}\left(\frac{dw_i}{dr}\right)^2 dr. \tag{B4}$$

The boundary conditions are that the radial stress vanishes at the free end,

$$\sigma_r^b = \frac{1}{r}\frac{\partial \chi}{\partial r} = 0 \quad \text{at} \quad r = R_I \text{ and } R_O. \tag{B5}$$

In addition, the radial and tangential stresses should be continuous at the boundary between the two regions. This gives four conditions for χ, namely that $\partial\chi/\partial r$ and $\partial^2\chi/\partial r^2$ are continuous at $r = R_L$ and R_S. Then a straightforward calculation leads to

$$P_1 = P_2 - \frac{E}{4}[F_2(R_L) - F_1(R_L)],$$

$$Q_1 = Q_2 - \frac{E}{2}[G_2(R_L) - G_1(R_L)] + \frac{ER_L^2}{4}[F_2(R_L) - F_1(R_L)],$$

$$P_2 = -\frac{E}{2(R_O^2 - R_I^2)}\left\{G_1(R_I) - G_1(R_L) + G_2(R_L) - G_2(R_S) + G_3(R_S) - G_3(R_O) - \frac{(R_I^2 - R_L^2)}{2}[F_1(R_L) - F_2(R_L)] + \frac{(R_O^2 - R_S^2)}{2}[F_3(R_S) - F_2(R_S)]\right\},$$

$$Q_2 = \frac{E}{2(R_O^2 - R_I^2)}\left\{R_O^2[G_1(R_I) - G_1(R_L) + G_2(R_L)] - R_I^2[G_2(R_S) - G_3(R_S) + G_3(R_O)] - \frac{R_O^2(R_I^2 - R_L^2)}{2}[F_1(R_L) - F_2(R_L)] + \frac{R_I^2(R_O^2 - R_S^2)}{2}[F_3(R_S) - F_2(R_S)]\right\},$$

$$P_3 = P_2 - \frac{E}{4}[F_2(R_S) - F_3(R_S)],$$

$$Q_3 = Q_2 - \frac{E}{4}[G_2(R_S) - G_3(R_S)] + \frac{ER_S^2}{4}[F_2(R_S) - F_3(R_S)]. \tag{B6}$$

The integral given by eqn (10) in Section 3 is now written with the above equations as

$$DC1w0 + tC3(w0)^3 + PC0 = 0, \tag{B7}$$

where

$$C0 = \frac{w_2(R_L)}{2\pi w0},$$

$$C1 = -\frac{4w_2(R_L)}{w0},$$

$$C3 = -\left\{\int_{R_I}^{R_L} \delta_{i1} + \int_{R_L}^{R_S} \delta_{i2} + \int_{R_S}^{R_O} \delta_{i3}\right\}\left[P_i + \frac{Q_i}{r^2} - \frac{E}{2r^2}G_i(r)\right]\left(\frac{1}{w0}\frac{dw_i}{dr}\right)^2 r\,dr. \tag{B8}$$